Inorg. Chem. **2006**, *45*, 6198–6204

A Topological Study of the Geometry of AF_6E Molecules: Weak and Inactive Lone Pairs

Julien Pilmé,[†] Edward A. Robinson,[‡] and Ronald J. Gillespie*[,§]

Department of Chemistry, McMaster University, Hamilton, Ontario L8S 4M1, Canada, Laboratoire de Chimie, UMR CNRS 5182, Ecole Normale Supérieure de Lyon, 46 Allée d'Italie, F-69364 Lyon Cedex 07, France, and 35 Beach Road West, Portishead, Bristol BS20 7HX, U.K.

Received December 23, 2005

The geometries of AF_6E molecules, which may have either an O_h or a C_{3v} geometry, have been studied by means of the electron localization function. Our results show that when the molecule has a C_{3v} geometry, there is a valence-shell monosynaptic V(A) basin corresponding to the presence of a lone pair in the valence shell of the central atom A. The population of this basin is, however, extensively delocalized so that the electron density has a core-valence basin character, which is consistent with an earlier suggestion of a weakly active lone pair that gives a C_{3v} distorted octahedral molecule rather than the valence-shell electron-pair repulsion predicted pentagonal-pyramid geometry. In contrast, the molecules with O_h geometry do not have a monosynaptic valence-shell basin, but they have a larger core. These results provide confirmation of a previous suggestion that in AX_6E (X = Cl, Br, I) molecules with the O_h geometry the ligands X are sufficiently closely packed around the central atom A so as to leave no space in the valence shell for the lone pair E, which remains part of the core. Among the corresponding fluorides, only BrF_6^- has the O_h geometry, while the others have the C_{3v} geometry because there is sufficient space in the valence shell to accommodate the lone pair, the presence of which distorts the O_h geometry to C_{3v}. The energies of the O_h and C_{3v} geometries have been shown to be very similar so the observed geometries are a consequence of a very fine balance between ligand–ligand repulsions and the energy gained by the expansion of the two nonbonding electrons into the valence shell.

Introduction

The geometry of molecules with seven electron pairs in the valence shell of a central atom cannot be predicted with certainty by the valence-shell electron-pair repulsion (VSEPR) model[1] for two reasons: (1) A pentagonal bipyramid (D_{5h}), a monocapped octahedron (C_{3v}), and a monocapped triangular prism (C_{2v}) are all predicted by the particles-on-a-sphere model depending on the force law assumed for the interaction between the particles. (2) Seven particles cannot be arranged on a sphere so as to all be equivalent and at equal distances from the center. In fact, all known main group AX_7 molecules, such as IF_7 and TeF_7^-, have a pentagonal-bipyramidal (D_{5h}) geometry with longer equatorial than axial bonds. Moreover, the only known AX_5E_2 molecules, IF_5^{2-}[2] and XeF_5^-,[3] have a pentagonal-bipyramidal arrangement of seven electron pairs, with the lone pairs in the axial positions giving a planar pentagonal geometry. So, it is reasonable to assume that AX_6E molecules would also have a pentagonal-bipyramidal arrangement of seven electron pairs, with the lone pair in an axial position giving a pentagonal-pyramidal molecule (Figure 1). However, many molecules of this type including the ions SnX_6^{4-}, PbX_6^{4-}, SbX_6^{3-}, BiX_6^{3-}, SeX_6^{2-}, and TeX_6^{2-}, where X = Cl, Br, or I, have a regular octahedral structure.[2] When X = F, ClF_6^-[4] and BrF_6^-[5] also have regular octahedral geometries, but the fluorides SeF_6^{2-},[6] IF_6^-,[5,7] and

* To whom correspondence should be addressed. E-mail: ronald.gillespie@sympatico.ca.
[†] Ecole Normale Supérieure de Lyon.
[‡] Portishead.
[§] McMaster University.

(1) Gillespie, R. J.; Nyholm, R. S. Q. *Rev. Chem. Soc.* **1957**, *11*, 339. Gillespie, R. J.; Hargittai, I. *The VSEPR Model of Molecular Geometry*; Allyn and Bacon: Boston, MA, 1991. Gillespie, R. J.; Popelier, P. L. A. *Chemical Bonding and Molecular Geometry*; Oxford University Press: Oxford, U.K., 2001.
(2) Christe, K. O.; Wilson, W. W.; Drake, G. W.; Dixon, D. A.; Boatz, J. A.; Gnann, R. Z. *J. Am. Chem. Soc.* **1998**, *120*, 4711.
(3) Christe, K. O.; Curtis, E. C.; Dixon, D. A.; Mercier, H. P.; Sanders, J. C. P.; Schrobilgen, G. J. *J. Am. Chem. Soc.* **1991**, *113*, 3351.
(4) Christe, K. O.; Wilson, W. W.; Chirakal, R. V.; Sanders, J. C. P.; Schrobilgen, G. J. *Inorg. Chem.* **1990**, *29*, 3506.
(5) Christe, K. O.; Wilson, W. W. *Inorg. Chem.* **1989**, *28*, 3275.

10.1021/ic052182+ CCC: $33.50
Published on Web 07/08/2006

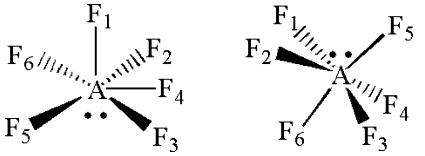

Figure 1. Pentagonal-bipyramidal C_{5v} (left) arrangement and C_{3v} distorted (right) arrangement of a AF_6E molecule.

XeF_6[8−12] have C_{3v} distorted "octahedral" geometries (Figure 1). However, no AX_6E molecules have the pentagonal-pyramidal structure.

In the octahedral molecules, it appears that the geometry is determined only by ligand−ligand repulsions and that the two nonbonding electrons have no influence on the geometry. These electrons have been described as a sterically inactive lone pair. It has been suggested[13] that they do not, in fact, form a lone pair in the valence shell of A but rather a spherical outer shell of the core. In the atomic orbital approximation, these electrons would be described as occupying a *n*s orbital and therefore having no influence on the geometry. Because the nonbonding electrons in the C_{3v} molecules have a smaller influence on the geometry than they have in a molecule with a pentagonal-pyramidal geometry, they have been described as a weakly active lone pair. It has been suggested,[13] therefore, that they could be described as a partial lone pair with the nonbonding electrons partly in the valence shell and partly in the core. In the O_h molecules AX_6E, X = Cl, Br, or I, the large halogen ligands may be regarded as close-packed around the central atom giving the octahedral geometry, leaving no space in the valence shell for the nonbonding electrons, which remain in an outer spherical shell of the core. Among the corresponding fluorides, only BrF_6^- has an octahedral geometry, but SeF_6^{2-}, TeF_6^{2-}, IF_6^-, and XeF_6 have C_{3v} geometries. Because these molecules have larger central atoms, it has been suggested[6,13,14] that the small fluorine ligands do not take up all of the available space in the valence shell, leaving space for at least some of the nonbonding electrons.

A very thorough and extensive ab initio study of XeF_6 and other AF_6E molecules has been done by Kaupp et al.[15] Dixon et al.[12] have also recently made high-level ab initio calculations for XeF_6. They found that the energy difference between the O_h and C_{3v} structures is very small and depends strongly on the balance between electron correlation, relativity, and basis set effects. Both of these groups found that the O_h structure has a very slightly lower energy than the C_{3v} structure. For example, Dixon et al. found that the O_h structure of XeF_6 is only 0.19 kcal below the C_{3v} structure at the CCSD(T)/CBS level using an approximate geometry for the C_{3v} structure. They predicted that with an optimized geometry the C_{3v} structure would probably become slightly lower in energy than the O_h one. Clearly, the energy difference between the O_h and C_{3v} structures is determined by some very subtle effects that require larger computational resources than are currently accessible. Not surprisingly, XeF_6 is a fluxional molecule, but it seems reasonable to suppose that the C_{3v} structures of the crystalline AF_6E ionic compounds are stabilized by anion−cation interactions.

The C_{3v} distortion is usually described as a pseudo-Jahn−Teller stabilization[15−18] from the O_h symmetry. Indeed, only the C_{3v} arrangement allows an interaction by symmetry between the frontier orbitals, whereas this overlap is forbidden in the O_h symmetry. Consequently, it has been suggested that the C_{3v} stabilization is due to the increase in the frontier orbital splitting. However, because the previous high-level calculations[12,15] have shown that electron correlation and relativistic effects have an influence on the symmetry of the ground state, the electronic structure of these molecules is clearly more complex than the understanding given by the qualitative molecular orbital model, which cannot be expected to provide a rationalization of the structures of AX_6E molecules.

The purpose of the work described in this paper was not to attempt to repeat previous work on AF_6E molecules or to come to a conclusion on the relative stability of C_{3v}/O_h but rather to provide a further understanding of the geometries of these molecules, in particular to see if the description of the O_h and C_{3v} geometries of these molecules given by the modified VSEPR model, as described by Seppelt et al.[6] and by Gillespie and Robinson,[13,14] is confirmed by the topological analysis of the electron localization function (ELF).[19,20] In particular, we have obtained further information on the nature of the "weak" lone pair postulated to explain the C_{3v} geometry in the VSEPR description of these molecules.

Computational Methods

Calculations have been performed at the hybrid Hartree−Fock (HF) density functional theory (DFT) B3LYP level[21,22] and the relativistic HF (RHF) method with the *Gaussian 03* software.[23] The standard all-electron basis set 6-311+G(2df) was employed for the atoms S, Cl, Ar, As, F, Se, Br, and Kr, while the 6-311G* basis set was used for the I atom and the DGDZVP[24,25] basis set for the Xe, Sb, and Te atoms. To allow for relativistic effects, the small-core (28 core electrons) relativistic effective core potential (RECP) of the Stuttgart/Köln group was also used for Sb, Te, I, and Xe atoms.[26] Only the valence electrons ($4s^24p^65s^24d^{10}5p^6$) were explicitly taken into account, and the valence orbitals were described with the standard cc-pVTZ-PP[26] basis set. We optimized the geometry of all of the molecules studied in both the O_h and C_{3v}

(6) Mahjoub, A. R.; Zhang, X.; Seppelt, K. *Chem.—Eur. J.* **1995**, *261*, 1.
(7) Christe, K. O.; Seppelt, K. *Angew. Chem., Int. Ed. Engl.* **1991**, *30*, 321.
(8) Bartell, L. S.; Gavin, R. M. *J. Chem. Phys.* **1968**, *48*, 2460.
(9) Bartell, L. S.; Gavin, R. M. *J. Chem. Phys.* **1968**, *48*, 2466.
(10) Cutler, J. N.; Bancroft, G. M.; Bozek, J. D.; Tan, K. H.; Schrobilgen, G. J. *J. Am. Chem. Soc.* **1991**, *113*, 9125.
(11) Pitzer, K. S.; Bernstein, L. S. *J. Chem. Phys.* **1975**, *63*, 3849.
(12) Dixon, D. A.; de Jong, W. A.; Peterson, K. A.; Christe, K. O.; Schrobilgen, G. J. *J. Am. Chem. Soc.* **2005**, *127*, 8627.
(13) Robinson, E. A.; Gillespie, R. J. *Inorg. Chem.* **2003**, *42*, 3865.
(14) Gillespie, R. J.; Robinson, E. A. *Chem. Soc. Rev.* **2005**, *34*, 396.
(15) Kaupp, M.; van Wüllen, C.; Franke, R.; Schmitz, F.; Kutzelnigg, W. *J. Am. Chem. Soc.* **1996**, *118*, 11939.
(16) Opïk, U.; Pryce, M. H. L. *Proc. R. Soc. London, Ser. A* **1957**, *A238*, 425.
(17) Bader, R. F. W. *Mol. Phys.* **1960**, *3*, 137.
(18) Seppelt, K. *Acc. Chem. Res.* **2003**, *36*, 147.
(19) Becke, A. D.; Edgecombe, K. E. *J. Chem. Phys.* **1990**, *92*, 5397.
(20) Silvi, B.; Savin, A. *Nature* **1994**, *371*, 683.
(21) Lee, C.; Yang, W.; Parr, R. G. *Phys. Rev. B* **1988**, *37*, 785.
(22) Becke, A. D. *J. Chem. Phys.* **1993**, *98*, 5648.

symmetries because these are the symmetries previously observed experimentally or found by high-level calculations.

All of the topological analyses were carried out from a Kohn−Sham wave function with the TopMoD package,[27] and the ELF isosurfaces have been visualized with the *Molekel* software.[28]

Topological Analysis

In a topological analysis,[20] a partitioning of the molecular space is achieved by the theory of dynamical systems. This partitioning gives a set of basins localized around the attractors (maxima) of the vector field of a scalar function. In the QTAIM theory,[2,29] this scalar function is the electron density and the basins (Ω) are associated with each of the atoms in the molecule. Atomic properties such as the atomic volume and the atomic population ($\bar{N}[\Omega]$) can then be calculated by integration over the basin defining an atom. Another relevant function is η, the ELF of Becke and Edgecombe,[19] which can be interpreted in terms of the excess kinetic energy due to the Pauli repulsion[30,31] or in terms of the probability of finding opposite-spin electron pairs.[32] ELF basins may be interpreted as those regions where there is a high probability of finding pairs of opposite-spin electrons, namely, the atomic cores and the bonding and nonbonding regions. The ELF topology has been extensively used for the analysis of chemical bonding or chemical reactivity.[33−40] The relationship of the ELF function to pair functions has been demonstrated,[32] but in contrast to the pair functions, ELF, which is defined to have values between 0 and 1, can be easily calculated and interpreted.

Core basins (if $Z > 2$) are labeled C(A). The valence basins are situated in the remaining space. Each valence basin that is connected to only one atomic center is called a monosynaptic basin and is labeled V(A). Each basin that is connected to two atomic centers is called a disynaptic basin and is labeled V(A,B). These basins closely match the nonbonding (lone-pair) and bonding domains of the VSEPR model,[1] and they may be considered to be a quantitative expression of these electron-pair domains. The population of a basin $\bar{N}(\Omega)$ can be calculated by integrating the one-electron density over the basin volume.

The closure relationship of the basin population operators enables a statistical analysis of the population to be made through the definitions of the variance of the basin population[41] (noted σ^2), which is a diagonal element of the covariance matrix.[42] The element of the covariance matrix between the populations of two given basins Ω_A and Ω_B is defined as $\mathrm{cov}(\Omega_A,\Omega_B) = \int\int_{\Omega_A}\int_{\Omega_B}\pi(\vec{r}_1,\vec{r}_2)\, d\vec{r}_1\, d\vec{r}_2 - \bar{N}(\Omega_A)\bar{N}(\Omega_B)$, where $\pi(\vec{r}_1,\vec{r}_2)$ is the spinless second-order density. The variance is interpreted as the population uncertainty, i.e., a measurement of the fluctuation for a given basin with all of the other basins, while the values of the covariance matrix elements are a measure of the correlation between the populations of two given basins.

Results and Discussion

The results of B3LYP (all-electron and RECP) calculations for both octahedral and C_{3v} symmetries are presented in Table 1 together with the experimentally determined structures. At the DFT level, a C_{3v} minimum is found for each of SeF_6^{2-}, TeF_6^{2-}, and IF_6^-, while AsF_6^{3-}, SbF_6^{3-}, SF_6^{2-}, ClF_6^-, BrF_6^-, ArF_6, and KrF_6 cannot be optimized in C_{3v} symmetry because in these molecules the B3LYP optimization leads to the O_h symmetries in all cases. The difference in energy between the C_{3v} and O_h symmetries was found to be very small, just as has been found in the previous high-level calculations of Kaupp et al.[15] and Dixon et al.[12] Our B3LYP geometry optimizations for BrF_6^-, SeF_6^{2-}, TeF_6^{2-}, and IF_6^- are in reasonable agreement with experiment, although only fair for XeF_6, for which the C_{3v} stationary point was a HF calculation because we were unable to find a B3LYP minimum. The optimized A−F distances are generally overestimated in comparison to the experimental values. However, the RECP optimizations for SbF_6^{3-}, TeF_6^{2-}, IF_6^-, and XeF_6 led to slightly shorter A−F distances (3−4 pm) and a larger angle F_1-A-F_3 than the all-electron calculations and are in better agreement with the experimental data.

From the VSEPR point of view, an AX_6E molecule is expected to have a pentagonal-pyramidal (C_{5v}) geometry,

(23) Frisch, M. J.; Trucks, G. W.; Schlegel, H. B.; Scuseria, G. E.; Robb, M. A.; Cheeseman, J. R.; Montgomery, J. A., Jr.; Vreven, T.; Kudin, K. N.; Burant, J. C.; Millam, J. M.; Iyengar, S. S.; Tomasi, J.; Barone, V.; Mennucci, B.; Cossi, M.; Scalmani, G.; Rega, N.; Petersson, G. A.; Nakatsuji, H.; Hada, M.; Ehara, M.; Toyota, K.; Fukuda, R.; Hasegawa, J.; Ishida, M.; Nakajima, T.; Honda, Y.; Kitao, O.; Nakai, H.; Klene, M.; Li, X.; Knox, J. E.; Hratchian, H. P.; Cross, J. B.; Bakken, V.; Adamo, C.; Jaramillo, J.; Gomperts, R.; Stratmann, R. E.; Yazyev, O.; Austin, A. J.; Cammi, R.; Pomelli, C.; Ochterski, J. W.; Ayala, P. Y.; Morokuma, K.; Voth, G. A.; Salvador, P.; Dannenberg, J. J.; Zakrzewski, V. G.; Dapprich, S.; Daniels, A. D.; Strain, M. C.; Farkas, O.; Malick, D. K.; Rabuck, A. D.; Raghavachari, K.; Foresman, J. B.; Ortiz, J. V.; Cui, Q.; Baboul, A. G.; Clifford, S.; Cioslowski, J.; Stefanov, B. B.; Liu, G.; Liashenko, A.; Piskorz, P.; Komaromi, I.; Martin, R. L.; Fox, D. J.; Keith, T.; Al-Laham, M. A.; Peng, C. Y.; Nanayakkara, A.; Challacombe, M.; Gill, P. M. W.; Johnson, B.; Chen, W.; Wong, M. W.; Gonzalez, C.; Pople, J. A. *Gaussian 03*, revision B.02; Gaussian, Inc.: Pittsburgh, PA, 2004.
(24) Godbout, N.; Salahub, D. R.; Andzelm, J.; Wimmer, E. J. *Can. J. Chem.* **1992**, *70*, 560.
(25) Andzelm, J.; Wimmer, E. *J. Chem. Phys.* **1992**, *96*, 1280.
(26) Peterson, K. A.; Figgen, D.; Goll, E.; Stoll, H.; Dolg, M. *J. Chem. Phys.* **2003**, *119*, 11113.
(27) Noury, S.; Krokidis, X.; Fuster, F.; Silvi, B. *Comput. Chem.* **1999**, *23*, 597.
(28) Flukiner, P.; Luthi, H. P.; Portman, S.; Weber, J. *Molekel*; Swiss Center for Scientific Computing: Manno, Switzerland, 2000−2002.
(29) Bader, R. F. W. *Atoms in Molecules: A Quantum Theory*; Oxford University Press: Oxford, U.K., 1990.
(30) Kohout, M.; Savin, A. *Int. J. Quantum Chem.* **1996**, *60*, 875.
(31) Savin, A.; Nesper, R.; Wengert, S.; Fässler, T. F. *Angew. Chem., Int. Ed. Engl.* **1997**, *36*, 1809.
(32) Silvi, B. *J. Phys. Chem. A* **2003**, *107*, 3081.
(33) Fuster, F.; Sevin, A.; Silvi, B. *J. Phys. Chem. A* **2000**, *104*, 852.
(34) Llusar, R.; Beltrán, A.; Andrés, J.; Noury, S.; Silvi, B. *J. Comput. Chem.* **1999**, *20*, 1517.
(35) Choukroun, R.; Donnadieu, B.; Zhao, J. S.; Cassoux, P.; Lepetit, C.; Silvi, B. *Organometallics* **2000**, *19*, 1901.
(36) Chesnut, D. B.; Bartolotti, L. *J. Chem. Phys.* **2000**, *253*, 1. Chesnut, D. B.; Bartolotti, L. *J. Chem. Phys.* **2000**, *257*, 171.
(37) Fressigné, C.; Maddaluno, J.; Marquez, A.; Giessner-Prettre, C. *J. Org. Chem.* **2001**, *65*, 8899.
(38) Gillespie, R. J.; Noury, S.; Pilmé, J.; Silvi, B. *Inorg. Chem.* **2004**, *43*, 3248.
(39) Noury, S.; Silvi, B.; Gillespie, R. J. *Inorg. Chem.* **2002**, *41*, 2164.
(40) Pilme, J.; Silvi, B.; Alikhani, E. A. *J. Phys. Chem. A* **2005**, *109*, 10028.
(41) Savin, A.; Silvi, B.; Colonna, F. *Can. J. Chem.* **1996**, *74*, 1088.
(42) Silvi, B. *Phys. Chem. Chem. Phys.* **2004**, *6*, 256.

Table 1. B3LYP Calculations: Relative Energies and Structural Parameters for AF_6E and XeF_5^- Molecules

molecule		r_{A-F_1} (pm), r_{A-F_3} (pm)	$A_{F_1-A-F_3}$ (deg)	ΔE^a	De[b]
PF_6^{3-}	oct	205.6	180.0		−2226.5
AsF_6^{3-}	oct	213.8	180.0		−2178.8
SbF_6^{3-}					
all-electron	oct	232.3	180.0		−2590.4
RECP	oct	229.8	180.0		−2845.6
SF_6^{2-}	oct	190.2	180.0		−1601.7
SeF_6^{2-}	C_{3v}	205.1 (203),[c] 190.7 (184)[c]	173.8 (172)[c]	0.0	−1721.3
	oct	197.8	180.0	1.7	−1719.6
TeF_6^{2-}					
all-electron	C_{3v}	222.7, 206.8	168.8	0.0	−1924.0
	oct	215.1	180.0	1.4	−1922.6
RECP	oct	212.0	180.0	0.0	−1936.1
	C_{3v}	218.9, 204.6	169.8	2.1	−1934.0
ClF_6^-	oct	182.6	180.0		−471.6
BrF_6^-	oct	189.6 (185)[d]	180.0 (180)[d]		−781.5
IF_6^-					
all-electron	C_{3v}	210.1, 197.4	164.7	0.0	−1084.1
	oct	204.6	180.0	7.8	−1076.3
RECP	oct	201.5	180.0	0.0	−1196.4
	C_{3v}	205.9 (201),[e] 196.4 (186)[e]	168.3 (164)[e]	4.8	−1191.6
ArF_6	oct	184.2	180.0		777.5
KrF_6	oct	186.8	180.0		319.6
XeF_6					
all-electron	oct	200.4	180.0	0.0	−123.8
	C_{3v}	197.1,[f] 183.6[f]	153.0[f]	94.3[g]	−29.5[g]
RECP	oct	195.8	180.0	0.0	−277.3
	C_{3v}	193.8[f] (191),[h] 180.3[f] (186)[h]	154.6[f]	88.0[g]	−189.3[g]
XeF_5^-					
all-electron	pp[i]	210.2	72.0		
RECP	pp[i]	206.7 (201.2)[j]	72.0		

[a] Relative energy in kJ/mol. [b] Binding energy in kJ/mol with respect to the $[A + 3F_2]^{n-}$ barrier; $n = 0$, 1, 2, or 3. [c] Experimental values from ref 6. [d] Reference 5. [e] Reference 7. [f] RHF optimized geometry. [g] B3LYP single point. [h] Reference 9. [i] Planar pentagonal geometry. [j] Reference 3.

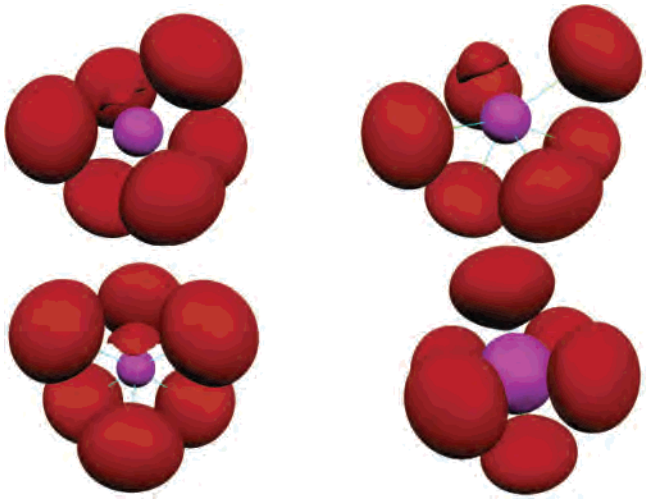

Figure 2. B3LYP localization domains of IF_6^- (top left; RECP, $\eta = 0.60$), XeF_6 (top right; all-electron, $\eta = 0.70$), SeF_6^{2-} (bottom left; all-electron, $\eta = 0.60$), and BrF_6^- (bottom right; all-electron, $\eta = 0.60$). Color code: magenta, core; red, valence monosynaptic.

with a lone pair in an axial position as we discussed in the Introduction (Figure 1). We have found a DFT minimum for the pentagonal-pyramidal geometry, but this is not the ground state because it has a very high energy with respect to the O_h structure. Indeed, the BrF_6^-, SeF_6^{2-}, IF_6^-, and XeF_6 molecules in C_{5v} symmetry are respectively 166.1, 135, 63.1, and 86.6 kJ/mol (all-electron) higher in energy than the octahedral structures.

Figure 2 displays the localization domains of IF_6^- (C_{3v}), BrF_6^- (O_h), SeF_6^{2-} (C_{3v}), and XeF_6 (C_{3v}).

In the octahedral structure, the only valence basins that are observed are the V(F) basin for each fluorine in addition to the large-core basin C(A) of the central atom. In contrast, in the C_{3v} symmetry, a supplementary valence-shell monosynaptic basin V(A) (nonbonding or lone pair) is localized between F_1, F_2, and F_5 (Figure 1). The topological structures calculated using both the RECP and the all-electron basis sets are quite similar. It is perhaps at first sight surprising that no disynaptic basins V(A,F) are observed in any of the molecules that we have studied. This is probably due to the strong polarity and great length (180−230 pm) of the bonds in these molecules.[39] It appears that the disynaptic (bonding) basin population decreases with increasing bond length, as shown by the V(A,F) populations of 1.45 and 0.95 electrons for BF_3 (D_{3h}) and PF_3 (C_{3v}), which have bond lengths of 131 and 159 pm, respectively (B3LYP/6-311+G(2d)), while their polarities are very similar, as expected from their electronegativities and as shown by their calculated fluorine AIM charges of −0.81 and −0.76, respectively.

Table 2 gives the ELF population analysis at the B3LYP level for all of the molecules studied. For TeF_6^{2-}, IF_6^-, and XeF_6, in addition to the analysis of the all-electron wave function, the RECP population analysis is also presented. Column 1 gives the core population $\bar{N}$[C(A)], and column 2 gives the core population excess Δ calculated with respect to the configurations [Ne] (10e), [Ar] d^{10} (28e), and [Kr] d^{10} (46e) and for the RECP core population (18e). For all of the C_{3v} structures, the core excess Δ is very small or generally slightly negative [0.15 for TeF_6^{2-}, −0.23 for IF_6^-, −0.12 for XeF_6 (RECP), and −0.43 for SeF_6^{2-} (all-electron)] and

Table 2. ELF Population Analysis of AF_6E Molecules at the B3LYP Level

molecule		$\bar{N}$[C(A)]	Δ^a	$\bar{N}$[V(A)]	σ^2[V(A)]	$q^{ELF}(A)^b$	$q^{ELF}(F_1)$,^{b} $q^{ELF}(F_3)^b$
PF_6^{3-}	oct	13.65	3.65[1]			1.35	−0.72
AsF_6^{3-}	oct	31.21	3.21[2]			1.79	−0.80
SbF_6^{3-}							
all-electron	oct	48.50	2.50[3]			2.50	−0.91
RECP	oct	20.39	2.39[4]			2.61	−0.93
SF_6^{2-}	oct	14.09	4.09[1]			1.91	−0.65
SeF_6^{2-}	C_{3v}	27.57	−0.43[2]	3.26	2.14	3.17	−0.96, −0.76
	oct	31.80	3.80[2]			2.20	−0.70
TeF_6^{2-}							
all-electron	C_{3v}	46.68	0.68[3]	2.53	1.89	2.79	−0.85, −0.74
	oct	49.34	3.34[3]			2.66	−0.77
RECP	C_{3v}	18.15	0.15[4]	2.73	1.97	3.11	−0.91, −0.79
	oct	21.0	3.00[4]			3.00	−0.83
ClF_6^-	oct	14.50	4.50[1]			2.50	−0.58
BrF_6^-	oct	32.26	4.26[2]			2.74	−0.62
IF_6^-							
all-electron	C_{3v}	46.15	0.15[3]	3.06	2.11	3.79	−0.90, −0.70
	oct	49.71	3.71[3]			3.29	−0.71
RECP	C_{3v}	17.77	−0.23[4]	3.04	2.14	4.19	−0.92, −0.80
	oct	20.98	2.98[4]			4.02	−0.83
ArF_6	oct	15.79	5.79[1]			2.21	−0.37
KrF_6	oct	33.76	5.76[2]			2.24	−0.37
XeF_6							
all-electron	C_{3v}	46.15	0.15[3]	3.81	1.91	4.04	−0.81, −0.54
	oct	51.03	4.03[3]			2.97	−0.49
RECP	C_{3v}	17.88	−0.12[4]	3.33	1.98	4.79	−0.86, −0.74
	oct	21.82	3.82[4]			4.18	−0.69
XeF_5^-							
all-electron		45.64	−0.36[3]	3.18	1.32	2.00	−0.60
RECP		17.53	−0.47[4]	3.03	1.35	2.41	−0.56

[a] The core population excess Δ is calculated with respect to the following configurations: (1) [Ne] (10 e), (2) [Ar]d^{10} (28 e), (3) [Kr]d^{10} (46 e), (4) RECP core population (18 e). [b] A charge: $q^{ELF}(A) = Z(A) - \bar{N}[C(A)] - \bar{N}[V(A)]$. Fluorine charge: $q^{ELF}(F_i) = Z(F) - \bar{N}[C(F_i)] - \bar{N}[V(F_i)]$.

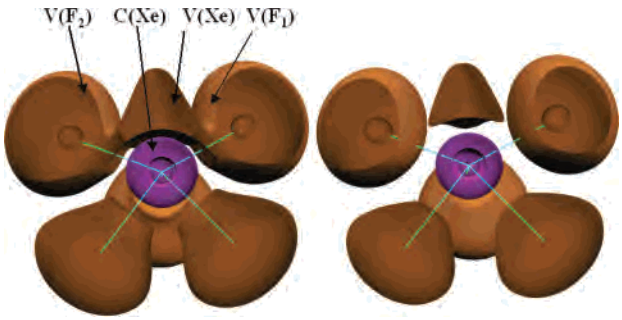

Figure 3. Split of the localization domains of the XeF_6 molecule in the C_{3v} symmetry (B3LYP, all-electron). Before the V(Xe)−V(F) domain separation (left; $\eta = 0.36$) and just after this separation (right; $\eta = 0.45$). Color code: magenta, core; orange, valence monosynaptic.

the valence shell basin V(A) has a population between 2.53 and 3.81 electrons. In addition, further information can be obtained by the hierarchical separation of the localization domains. Figure 3 displays the localization domains for XeF_6 for two ELF values (all-electron).

We see that the core−valence separation occurs well before the separation of the V(A) and V(F) domains, showing that the core electrons are much more localized than the V(F) and V(A) domains, which is consistent with the stability of the d^{10} configuration of the core in XeF_6.

For the O_h molecules, there is no monosynaptic basin and the core excess charge is correspondingly much larger, ranging from 2.5 to 5.79 electrons. Because the O_h molecules have no V(A) basin, the electrons that are in the V(A) basin in the C_{3v} molecules are found in the core of the O_h molecules, in agreement with the earlier suggestion that the nonbonding electrons remain in the core. The electrons that are not transferred to the fluorine ligands, and which would conventionally be regarded as nonbonding electrons, remain in the core in the O_h molecules or are shared between the core and the valence shell of A in the C_{3v} molecules but are principally in the valence shell because the core excess is quite small.

To understand the distribution of the populations, it is necessary to consider the variance σ^2 quantity of the V(A) population, which is given in Table 2. This variance appears large (close to 2) in each C_{3v} case, which signifies strong charge fluctuations into the valence V(A) and V(F) basins but also between the core and valence domains. In particular, the covariance matrix element between the C(A) and V(A) basin populations is negatively large (> -0.80), indicating a large density fluctuation between C(A) and V(A). For example, the covariance matrix element of −0.83 between V(Se) and C(Se) basins of SeF_6^{2-} is much larger than the value found for other related molecules such as ClF_5, where the covariance element between V(Cl) and C(Cl) basins is only −0.21. This extensive delocalization between the V(A) population and the core population of the AF_6E systems suggests an ambivalent core−valence character for the valence density. That the V(A) population cannot be clearly separated from the core population is consistent with the idea that it is less effective than a full lone pair; in other words, it is only partially active.

An ELF analysis of IF_6^- in the high-energy C_{5v} pentagonal-bipyramidal symmetry was carried out to make a comparison with the ELF analysis of the O_h and C_{3v} molecules. The

Table 3. B3LYP Calculations: Calculated Structural Parameters of the C_{3v} Molecules with Respect to the Fluorine Numbering Given in Figure 1

	distances (pm)			angle (deg)			
molecule (C_{3v})	F_1-F_2 (long−long)	F_2-F_6 (long−short)	F_3-F_4 (short−short)	F_1-A-F_2 (long−long)	F_2-A-F_6 (long−short)	F_3-A-F_4 (short−short)	vol.(A)[a]
SeF_6^{2-}	303.4	277.9	261.7	95.4	88.8	86.7	82.2
TeF_6^{2-}							
all-electron	340.8	296.6	277.9	99.9	87.3	84.4	122.7
RECP	332.9	293.5	276.0	98.9	87.6	84.8	76.0
IF_6^-							
all-electron	331.3	275.6	263.0	104.1	85.1	83.5	120.8
RECP	316.9	276.4	264.5	100.6	86.7	84.6	70.0
XeF_6							
all-electron	331.0	240.5	239.4	114.2	78.2	81.4	131.2
RECP	323.6	238.9	235.5	113.0	79.3	81.6	84.9

[a] Atomic volume (au) of the central atom from an AIM analysis.

energy of this structure is high, presumably because of the strong repulsions between the five ligands in the equatorial plane. In the C_{5v} symmetry, the population analysis shows one single monosynaptic basin on one side of the pentagonal plane of the fluorine ligands with a population of V(I) = 2.25 and a weak variance $\sigma^2[V(A)] = 1.13$. These results and the rather small covariance matrix element between C(I) and V(I) indicate a well-localized core−valence population and a fully active lone pair from the VSEPR point of view.[13,14]

Table 3 shows the geometrical parameters and the atomic volumes of the central atom obtained by an AIM analysis for each C_{3v} structure. The greater length of the A−F bonds surrounding the V(A) basin and the increased F−A−F angles are consistent with the repulsions exerted by the electrons in this basin with the surrounding ligands. It is interesting that the other three bonds decrease in length so that the average bond length remains almost the same as that in the corresponding molecule with O_h symmetry. The extent of the deformation from O_h to C_{3v} increases from BrF_6^- to SeF_6^{2-}, from SeF_6^{2-} to TeF_6^{2-}, and from TeF_6^{2-} to XeF_6 (Tables 1 and 3), that is, in each case with the increasing size of the central atom as shown by the atomic volumes obtained by an AIM analysis (Table 3).

With increasing size of the central atom, there is more space in the valence shell for the nonbonding electrons to expand into and decreased repulsion between the ligands, causing the bonds surrounding the lone pair to increase in length and the angles they make with the lone pair and the angles they make with each other to increase. Overall, it appears that in the AF_6E molecules there is a very fine balance between ligand−ligand repulsion, which would give the O_h geometry, and the tendency of the nonbonding electrons to expand from the core into the valence shell, thereby minimizing their energy, or, in other words, to move from a small highly localized s orbital to a larger and less localized sp hybrid orbital.

Finally, we have made an ELF analysis of the XeF_5^- molecule, which has the VSEPR-predicted planar pentagonal geometry[3] in order to compare it with XeF_6. The calculated geometry of XeF_5^- [3,12,43] was found to be planar pentagonal

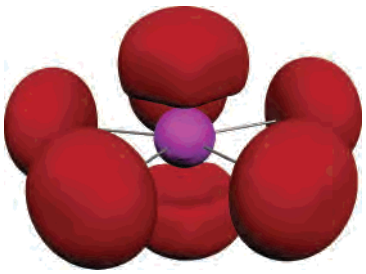

Figure 4. Localization domains of the XeF_5^- molecule (B3LYP, all-electron optimized, $\eta = 0.74$). Color code: magenta, core; red, valence monosynaptic.

(D_{5h}), in agreement with experiment.[3] The calculated bond length was found to be 206.7 pm (Table 1) compared with the high-level calculation of Dixon et al.[12] (203.4 pm) and the observed length of 201.2 pm[3]. Both the calculated and observed bond lengths are greater than the calculated and experimental lengths of the longer bonds in XeF_6, which is consistent with the presence of two lone pairs rather than just one. The results of the ELF analysis (Table 2) are very similar for the all-electron and RECP calculations. The ELF topology (Figure 4) displays two nonbonding basins V(Xe), one above and one below the equatorial plane.

The population of each V(Xe) basin is greater than 2, as for the single V(Xe) basin in XeF_6, and the variance and covariance indicate large fluctuations involving the valence basins V(F) and V(Xe). The core population excess has a small deficit so the core is close to the [Kr] d^{10} configuration, and the valence basins are primarily due to the $5s^25p^6$ electrons, as for XeF_6. Clearly, the type of distortion observed in the C_{3v} AF_6E molecules is not possible for AF_5E_2 molecules. The only possibility for a molecule of this type to have two equivalent lone pairs is to have a pentagonal-bipyramidal arrangement of seven electron pairs with the two lone pairs in the axial positions, which are the less crowded axial positions.

Conclusions

Our work has provided clear evidence that in AF_6E molecules with a C_{3v} geometry there is a monosynaptic basin V(A) in the valence shell of the central atom A that is responsible for the deformation of the molecule from O_h to C_{3v} symmetry. The lone pair in the VSEPR model is the equivalent of the ELF V(A) basin. This basin has a

(43) Fleurat-Lessard, P.; Durupthy, O.; Volatron, F. *Chem. Phys. Lett.* **2002**, *363*, 505.

population of more than two electrons but has large fluctuations with the valence V(F) basins, that is, with the fluorine valence electrons, and also with the core, so these electrons have an ambivalent core−valence character. This conclusion is consistent with the earlier proposal that the VSEPR lone pair is only a partial lone pair with some of its electron density in the valence shell and some in the core.

Our study shows that the geometry of the AF_6E molecules is determined by a very fine balance between the energy associated with ligand−ligand repulsion and that associated with the expansion of the nonbonding electrons from the core into the valence shell. In molecules in which the central atom is small enough, six fluorine ligands are essentially close-packed around the central atom so that there is no space available in the valence shell for the lone pair. For larger central atoms, the fluorine ligands are not quite close-packed so that there is some space for the nonbonding density to decrease its energy by expanding from the tight core to the less dense valence shell while at the same time distorting the octahedral geometry. It appears that AX_6E molecules with larger ligands such as Cl always have O_h geometry determined by ligand−ligand repulsion in which the two nonbonding electrons remain as an outer shell of the core. Our topological analysis of the ELF provides a qualitative rationalization of the O_h and C_{3v} structures of AF_6E molecules, which is consistent with the VSEPR model as modified by Seppelt et al.[6] and by Gillespie and Robinson.[13,14]

Acknowledgment. The authors gratefully thank one of the reviewers for his constructive comments on the effective core potential calculations.

IC052182+